

N78-24065

EBF NOISE REDUCTION THROUGH NOZZLE/FLAP POSITIONING*

Y. Kadman and K.L. Chandiramani
Bolt Beranek and Newman Inc.

SUMMARY

Results are presented of an experimental and analytical study of the dependence of Externally Blown Flap (EBF) noise on the relative position and shape of engine exhaust nozzle. Tests, conducted on a 1/15 scale model of a triple-slotted EBF system, indicate that a significant reduction (of up to 10 to 15 dB for no forward speed case and of up to 5 to 10 dB for forward speed case) is possible in the low frequency (around 63 Hz) region of the noise spectrum of the full scale device for small nozzle/flap separation distances. The overall acoustic performance, measured in PNdB, does not exhibit significant reductions. The analysis of the EBF noise is carried out for two limiting cases: (1) a turbulent jet being turned by a rigid corner, and (2) an isolated airfoil in a free jet. The analytical results also suggest that low frequency noise can be reduced by placing the nozzle close to the flow-turning elements.

INTRODUCTION

The noise from an integrated propulsive lift system arises from the engine and from the exhaust flow interacting with lift-augmenting flaps. Noise goals established for jet-powered STOL aircraft incorporating the propulsive lift concepts of under-the-wing externally blown flap (EBF), over-the-wing (OTW) blown flap (Coanda flap), internally blown flap, augmentor wing, or modifications of the above concepts require that the noise from the exhaust flow/lifting surface interactions be reduced substantially. Since muffling of these sources is not feasible, the generation of noise must be minimized. This requires an understanding of how noise is generated by turbulent flow interacting with flap-like surfaces, and what physical parameters (such as jet velocity, eddy size, etc.) affect the noise. Such an understanding is now sufficiently in hand to allow one to systematically seek methods for modifying the appropriate physical parameters in order to accomplish a reduced source level. However, one must be constrained in this pursuit by the fundamental necessity of maintaining adequate lift augmentation of the engine/flap system.

It is within these constraints that the present effort was undertaken to explore the effect of one parameter - the nozzle/flap separation - on the acoustic and aerodynamic performance of an EBF system.

*The above work was supported by contract from the NASA Lewis Research Center.

The experimental part of this effort was carried on a 1/15 scale model of a triple-slotted EBF system. The acoustic performance of the model was measured for a range of X/D from 0 to 3. Two exhaust nozzles - one round and one rectangular (Aspect ratio = 3.5) - were tested. All the acoustic data were compared at constant lift force.

The test results show that a reduction of up to 15 dB is possible in the low frequency (around 63 Hz) region of the noise spectrum of the full scale device for small nozzle/flap separation distances. The overall acoustic performance, when measured in PNdB, did not exhibit significant reductions.

The achieved large reductions of low frequency noise are considered important since one of the main problems associated with EBF systems is the high levels of noise and vibration inside the aircraft.

The analysis of the EBF noise problem was carried out for two limiting cases. The first case is that of a turbulent jet being turned by a rigid corner, and the second case is that of an isolated airfoil in a free jet.

The results of the analysis for both cases show that reduction of low frequency noise can be achieved by placing the nozzle close to the flow-turning elements.

Flap noise for EBF systems is dominated by three noise source mechanisms:

- Fluctuating forces on the whole flap (i.e., large scale fluctuations)
- Small scale pressure fluctuations at the leading edge of those flaps exposed to high velocity
- Trailing-edge noise from the flaps turbulent boundary layer and wake.

Secondary mechanisms are thought to be reflections of jet noise and surface-generated flow noise.

We expect the large scale fluctuations to determine the low frequency noise under investigation.

EXPERIMENTAL STUDY

Facility, Model and Instrumentation

The experimental phase of this effort was carried out in BBN's large wind tunnel facility in Cambridge, Massachusetts. For these experiments, the wind tunnel was fitted with a 28- by 40-in. nozzle which allows open jet velocities of up to 92 m/s (300 ft/sec). A compressor, with flow capacity of 3 m³/min (6000 ft³/min) at 103 400 Pa (15 psi) overpressure, supplied the high pressure air to the propulsive nozzle. A muffler on the high pressure line assured quiet flow to the EBF model. The tunnel test chamber was in the anechoic mode of operation. A detailed description of this high performance acoustic/aerodynamic test facility is given in reference 1.

The EBF model used in these tests was a triple-slotted type with 0.4-m (16-in.) flap span. Figure 1 is a drawing of the flap arrangement, showing both the takeoff (0° - 20° - 40°) and landing (15° - 35° - 50°) flap configurations. Only the takeoff configuration was tested in these series of experiments.

The model is a 1/15 scale model of an inboard engine nacelle and wing section designed and tested previously by NASA Langley Research Center. Table I summarizes the important dimensions.

The size of the nozzles that simulated the engine jet was arrived at by assuming that the full scale engine will produce 44 480 N (10 000 lb) of thrust at engine jet velocity of 244 m/sec (800 ft/sec) (pressure ratio of 1.35).

For cold flow of air, the above requirements will dictate a full scale nozzle area of 0.62 m^2 (6.67 ft^2) or a diameter of 0.89 m (35 in.). The model nozzle area will then be 0.003 m^2 (4.4 in^2).

Two nozzles were tested, a circular one, having a diameter of 0.06 m (2.37 in.) and a rectangular one, 0.03 by 0.1 m (1.12 by 3.9 in.), having an aspect ratio of 3.5. The maximum thrust that these equal area nozzles can develop at jet speeds of 244 m/sec (800 ft/sec) is 198 N (44.5 lb).

For the experiments, the EBF model was mounted on an extension of the wind tunnel nozzle floor and the high pressure air was ducted to the propulsive nozzle through an airfoil shaped duct so that interference between the main tunnel jet and ducting would be kept to a minimum. The location of the EBF model with respect to the stationary nozzle was varied by using the X-Y table, and an additional rotating table was used to adjust the angle of attack.

The instrumentation used in the tests consisted of two Band K 1/4 in. type 4135 microphones, one located 2.4 m (8 ft) below the wing and the other at an angle of 22° below the wing planform, at a distance of 3.05 m (10 ft). This second location corresponds to a side line test point as defined in reference 2.

Test Description

Two series of tests - one static and the other with forward speed - were performed. The investigation was confined to the range $X/D = 0$ to 3, with Y/D between 1/2 and 1. Larger values of Y/D are impractical since part of the flow misses the flaps and the lift decreases drastically.

The forward speed tests were performed with simulated forward velocity of 44 m/sec (145 ft/sec) and nozzle flow velocity of 152 m/sec (500 ft/sec) and 192 m/sec (630 ft/sec). All tests were carried out with the round nozzle and then repeated with the rectangular nozzle.

Criteria for EBF Performance Evaluation

The basic premise that underlies the present effort is that when a parametric noise study of a propulsive lift device is conducted, the results should be compared at constant lift force. Although a more comprehensive evaluation scheme that includes power requirements and the size of the various elements

of the system may be more useful, the constant-lift comparison is a first step in that direction.

Since the lift coefficient of different systems - and even of the same system under different geometric conditions - vary, the lift force was corrected in all tests to 198 N (44.5 lb) - which corresponds to the maximum possible lift force which can be obtained from the nozzles used at 244 m/sec (800 ft/sec). This value is somewhat arbitrary but it only serves as a common basis for comparison of the acoustic performance.

The effects of the lift corrections on the noise generated by the EBF model was computed by using scaling laws. One has two options of calculating the effects of these lift corrections on the noise. The first is to assume increased jet speed (and a higher pressure ratio) and the second is to increase nozzle area at a constant jet speed.

The thrust, or lift, and the noise from an EBF obey approximately the following:

$$\text{Thrust} \propto (\text{nozzle area}) (\text{jet velocity})^2$$

$$\text{Noise} \propto (\text{nozzle area}) (\text{jet velocity})^6$$

Doubling of the thrust, if achieved by increasing the velocity by a factor of $\sqrt{2}$, will "cost" 9 dB in additional noise, whereas by doubling the nozzle area the price will be only 3 dB.

It was decided therefore that the lift correction will be done at constant velocity (244 m/sec (800 ft/sec)) for all nozzle/flap configurations.

It should be noted here that the above procedure contains the implicit assumption that the lift coefficient C_L does not change with the nozzle area increase, but this is true only for small area changes. If the velocity is manipulated to increase the lift, no such assumption has to be made.

The implications of these lift correction methods on the power plant of the aircraft and the relative merit of each needs further study.

Test Results

Table II summarizes the predicted community noise in two locations, fly-over and sideline - both at a distance of 152 m (500 ft) from a 88 960-N (20 000-lb) thrust engine. Inspection of the table shows that when the noise is measured in PNdB, the acoustic performance of the EBF improves as one progresses to larger X/D. One should note, however, that the differences between the lowest and highest PNdB values are small (on the order of 2 dB or less) and are comparable to the experimental spread.

The individual pressure spectra for all of the 64 cases indicated in table II are reported in reference 3. Here, only a few selected spectra are displayed in figures 2 through 7. As in table I, the spectra refer to the full

scale situation (distance of 152 m (500 ft) from a 88 960-N (20 000-lb) thrust engine) and were obtained from the model spectra by the following procedure:

$$\text{SPL}_F(f_F) = \text{SPL}_M(f_M) + 60 \log \frac{U_{J,F}}{U_{J,M}} - 20 \log \frac{r_F}{r_M} + \log \frac{A_F}{A_M} \quad (1)$$

$$\frac{f_F}{f_M} = \frac{U_{J,F}}{U_{J,M}} \frac{d_M}{d_F} \quad (2)$$

Here, subscripts F and M refer to the full scale and model variables, SPL is the sound pressure level, f is the frequency, U_J is the jet velocity, r is the distance to the observation point, A is the nozzle area and d is the characteristic nozzle dimension.

Each of the figures 2 through 7 shows the variation in the noise level as a function of the nozzle/flap separation for a constant Y/D value. As mentioned before, the flaps were set at takeoff configuration (0° - 20° - 40°). Figures 2, 3, and 4 refer to the case of no forward speed, whereas figures 5, 6, and 7 refer to the case of a forward speed of 44 m/sec (145 ft/sec) for the same configurations.

The effect of nozzle/flap separation is evidenced clearly in the low frequency region of these spectra - a region which contributes little to the PNdB scale. The range of variation spans about 15 dB with no forward velocity and about 10 dB with forward velocity, and offers promise for significant alleviation of the interior noise and vibration problems.

The X/D dependence of overall noise (in PNdB) and of low frequency noise in one octave band (31.5 Hz to 63 Hz) is compared in figures 8 and 9 for the configurations selected for figures 2 through 7. Figure 8 shows the comparison for the case of no forward speed, and figure 9 shows the comparison for the case of a forward speed of 44 m/sec (145 ft/sec). As is evident from these figures, the reduction in low frequency noise with lower X/D is significantly larger than the associated slight increase in overall noise.

The nozzle shape did not seem to affect the noise. Some improvement in the low frequency region was detected but further study is needed to confirm these trends.

The effect of forward velocity was also found to be about the same on both nozzle shapes and, in general, reduced the noise by about 2 to 5 dB. As reported earlier (ref. 4), forward speed effects depend on the flap angles and, in general, do not reduce the noise by what may be expected from relative velocity arguments.

ANALYTICAL STUDIES

Predominant EBF noise generation mechanisms are dipole-like force fluctuations of the entire flap or fluctuations at the leading edge. Additional

sources, especially in the high frequency range occur at the trailing edge of the flaps. In the present effort, the analytical studies of the EBF noise were carried out on two limiting cases: (1) sound radiated by gross turning forces due to a turbulent jet being turned by a rigid corner, and (2) sound radiated by fluctuating lift at the leading edge of a thin isolated airfoil in a free jet.

These analyses are described in detail in reference 3. Here, we merely outline the basic ideas behind the analyses and present the calculated results.

Sound from Fluctuations in Gross Turning Forces

The EBF configuration is modelled as a simple smoothly faired corner with a jet against the concave part of the corner (fig. 10). It is assumed that in turning the corner, the only major change suffered by the total momentum flux across the jet cross-section is the change in its direction by angle ψ , with no substantial change in its magnitude or in its various statistics. On the basis of this assumption, the spectral density $\Phi_F(\omega)$ of the fluctuating force experienced by the flap is related to the spectral density $\Phi_M(\omega)$ of the fluctuating momentum flux in the flow direction by:

$$\Phi_F(\omega) = \Phi_M(\omega) \left\{ 2 \sin\left(\frac{\psi}{2}\right) \right\}^2, \quad (3)$$

where ψ is the turning angle of the flow. The above relation is likely to be valid only for large eddies, i.e., for low frequencies.

Next, the experimental data for round, subsonic jets (refs. 5 through 8) are used to estimate $\Phi_M(\omega)$ for various values of the dimensionless parameter X/D , where X is the axial location of the turning point and D is the nozzle diameter. For a given value of X/D , $\Phi_M(\omega)$ is a function of the flow dynamic head, the mean velocity profile; the spectral density of the fluctuating velocity in the axial direction; and a typical correlation area over the jet cross section, of the axial velocity fluctuations.

Finally, for estimating the noise radiated to the observation point \underline{r} , the fluctuating force on the flap is modelled as a whole-body, coherent, acoustic dipole source, possibly compact. Spectral density $\Phi_p(\underline{r}, \omega)$ of the radiated pressure is given by:

$$\Phi_p(\underline{r}, \omega) = \frac{\Phi_F(\omega)}{16\pi^2 r^2} \frac{k_a^2}{1 + k_a^2 b^2} D(\theta), \quad (4)$$

where k_a is the acoustic wavenumber at frequency ω , $D(\theta)$ is the directivity factor equal to $\cos^2\theta$ when θ is referred to the force axis and b is a typical dimension (semi-chord) of the source.

Figure 11 shows the estimated noise for the following conditions: nozzle diameter $D = 0.9$ m (3 ft); flap $X/D = 2, 4, 6$; turning angle $\psi = 60^\circ$; exit velocity = 213 m/sec (700 ft/sec), observation point 152 m (500 ft) radius (flyover).

Sound from Fluctuating Lift at Leading Edge

An airfoil of chord $2b$ and infinite span is considered to lie in a round turbulent jet (see sketch in fig. 12). The airfoil is assumed to lie in the x - y plane (i.e., $z = 0$). Its leading edge coincides with the x -axis and is at a distance X downstream of the jet nozzle.

A typical wave of fluctuating velocity $w(x, y, t)$ in the vertical z direction in the jet impinges on the airfoil and creates a corresponding wave of fluctuating lift on the airfoil, concentrated mainly at the leading edge. The velocity wave is given by:

$$w(x, y, t) = w_0 \exp \{i(k_1 x + k_2 y - \omega t)\} \quad , \quad (5)$$

and the corresponding lift $L(y, t)$ (of dimension force/length) is given by:

$$L(y, t) = 2\pi\rho b w_0 U T\left(\frac{\omega}{U}, k_2\right) \exp \{i(k_2 y - \omega t)\} \quad , \quad (6)$$

where w_0 is the amplitude of the incident upwash wave, k_1 and k_2 are the wave-number components of the wave, ρ is the medium density, $U = \omega/k_1$ is the mean velocity of the jet (dependent on the nozzle/airfoil separation X , and on the spanwise direction y) and $T(k_1, k_2)$ is the dimensionless response function (taken from ref. 8).

The experimental data of references 5 through 8 are used again to generate a statistical model of the wavenumber spectrum $\Phi_w(k_1, k_2)$ of the upwash disturbance and the corresponding spectrum $\Phi_T(k_2)$ of the leading edge fluctuations.

Finally, the radiated noise is calculated on the basis of regarding the leading edge lift fluctuations as statistically independent distribution of point dipoles of spanwise varying dipole strength. For high frequencies (for which $2b/\lambda > 1$, $\lambda =$ acoustic wavelength) a correction factor similar to that in equation 4 accounting for noncompact nature of lift distribution in the chordwise direction (only) is introduced.

Figure 12 shows the estimated noise for the following conditions: nozzle diameter $D = 0.9$ m (3 ft); chord $2b = 0.9$ m (3 ft); $X/D = 2, 4, 7.5, 10$; exit velocity = 244 m/sec (800 ft/sec); observation point 152 m (500 ft) radius (flyover).

Discussion

Both figures 11 and 12 indicate the same trend for low frequencies, i.e., less noise for closer nozzle/flap separations. For higher frequencies both the

figures indicate trends not suggested by experimental data. Figure 11 suggests higher high frequency noise for larger X/D, contrary to experiments. The assumption, and elementary estimation, of the whole body force is undoubtedly not valid for high frequencies where a typical eddy size is smaller than the flap dimensions. Although high frequency noise is seen to be less dependent on X/D in figure 13, the noise levels estimated are higher than those indicated by data. Likely reasons for higher estimated noise are: (1) In the approximate calculations performed, adequate account could not be taken of relatively rapid decay, with high $|k_2|$, of the lift response function $|T(k_1, k_2)|$ (this aspect is of less critical importance at lower frequencies). (2) $T(k_1, k_2)$ of reference 9 (and of related work) is based on the assumption that the impinging gust is infinitely extended in the z direction. Such an assumption may not be valid for small scale jet turbulence involved at higher frequencies.

CONCLUSIONS

The noise output of an EBF system in takeoff configuration was shown to be strongly dependent on the flap/nozzle configuration only at the low frequency region on the spectrum. The high frequency region, which dominates the various measures of community noise levels is only weakly affected by the nozzle/flap separation or the nozzle shape.

It is found that simple analytical models produce good approximations and trend predictions for the so-called "whole body dipole" noise source of an EBF system. This source dominates in the low frequency part of the spectrum and presents severe noise and vibration problems to the aircraft.

REFERENCES

1. Kadman, Y. and Hayden, R.E.: Design and Performance of High-Speed Free-Jet Acoustic Wind Tunnel. AIAA Paper 75-531, Hampton, Va., 1975.
2. Noise Standards: Aircraft Type and Airworthiness Certification. Federal Aviation Regulations, pt. 36, FAA, June 1974.
3. Kadman, Y., *et al.*: Exploratory Study of EBF Noise Reduction through Nozzle/Flap Positioning. BBN Report No. 2894, January 1976.
4. Dorsh, R.E.: Externally Blown Flap Noise Research. SAE Air Transportation Meeting, Dallas, Texas, 1974.
5. Laurence, J.C.: Intensity, Scale, and Spectra of Turbulence in Mixing Region of a Free Subsonic Jet. NACA Report 1292, 1956.
6. Bradshaw, P., Ferriss, D.H., and Johnson, R.F.: Turbulence in the Noise-Producing Region of a Circular Jet. AGARD Report 450, April 1963.
7. Wooten, D.C., *et al.*: A Study of the Structure of Jet Turbulence Producing Jet Noise. NASA CR-1836, July 1971.
8. Davies, P.O.A.L., Fisher, M.J. and Barratt, M.J.: The Characteristics of the Turbulence in the Mixing Region of a Round Jet. *J. of Fluid Mechanics*, 15, 1963.
9. Filotas, Y.T.: Theory of Airfoil Response in a Gusty Atmosphere, Part I - Aerodynamic Transfer Function. UTIAS Report No. 139, October 1969.

TABLE I.- EBF MODEL AND FULL SCALE DIMENSIONS

	Wing chord at inboard nacelle		First flap chord		Second flap chord		Third flap chord	
	m	in.	m	in.	m	in.	m	in.
Full scale aircraft	153	3.87	22.96	0.58	30.6	0.78	34.43	0.87
Model	10.2	.26	1.53	.04	2.04	.05	2.30	.06

TABLE II.- EBF NOISE AT CONSTANT LIFT (IN PNdB)

[88 960-N (20 000-1b) thrust engine at 152 m (500 ft) distance; $U_j = 244$ m/sec (800 ft/sec). Lift corrections performed by changes in nozzle area]

No Forward Speed								
Round Nozzle					Rectangular Nozzle			
Flyover		Sideline			Flyover		Sideline	
X/D	Y/D		Y/D		Y/D		Y/D	
	1/2	1	1/2	1	1/2	1	1/2	1
0	100.4	99.4	96.2	96.4	100.8	96.8	95.2	96.1
1	99.9	98.5	95.8	96.0	99.4	96.1	94.8	95.7
2	99.4	97.6	95.3	95.6	98.0	95.5	94.4	95.4
3	98.8	96.8	94.8	95.2	96.0	94.8	94.0	95.1

With Forward Speed $U_\infty = 44$ m/sec (145 ft/sec)								
Round Nozzle					Rectangular Nozzle			
Flyover		Sideline			Flyover		Sideline	
X/D	Y/D		Y/D		Y/D		Y/D	
	1/2	1	1/2	1	1/2	1	1/2	1
0	98.6	98.3	96.8	96.3	99.5	98.4	96.9	94.8
1	97.3	96.9	94.9	94.7	99.0	97.0	94.8	93.9
2	97.0	96.0	93.9	93.5	98.2	95.8	94.1	93.1
3	96.3	95.2	93.2	92.8	97.0	95.3	93.9	92.7

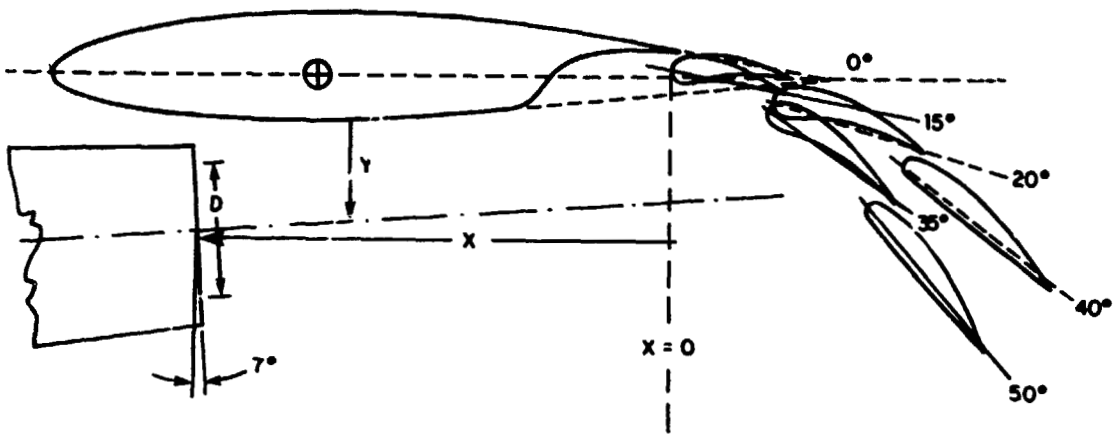


Figure 1.- EBF model geometry.

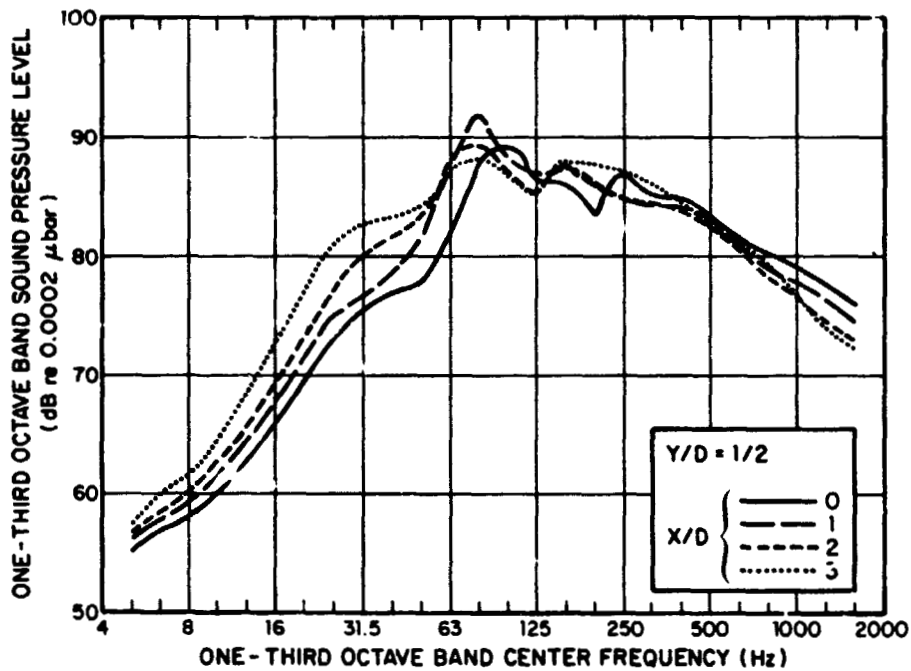


Figure 2.- Flyover noise spectra. Round nozzle; no forward speed; $U_j = 244$ m/s (800 ft/sec).

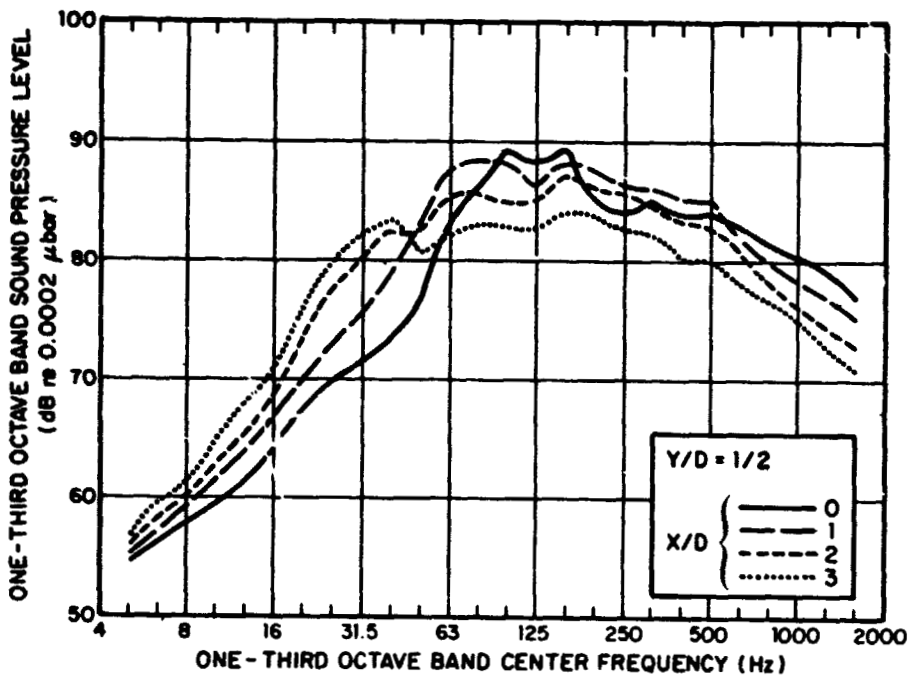


Figure 3.- Flyover noise spectra. Rectangular nozzle; no forward speed; $U_J = 244$ m/s (800 ft/sec).

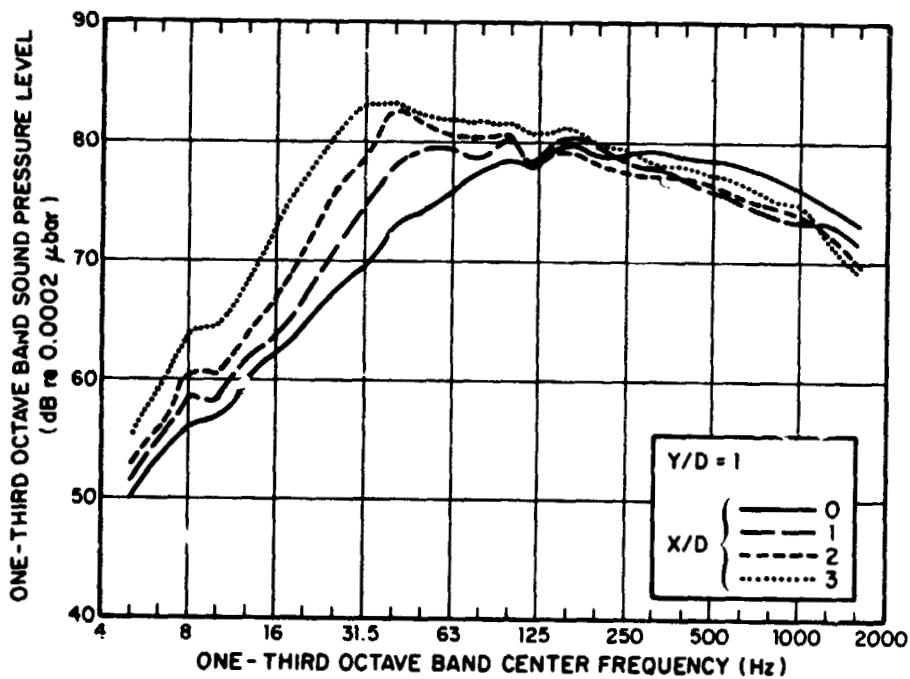


Figure 4.- Sideline noise spectra. Rectangular nozzle; no forward speed; $U_J = 244$ m/s (800 ft/sec).

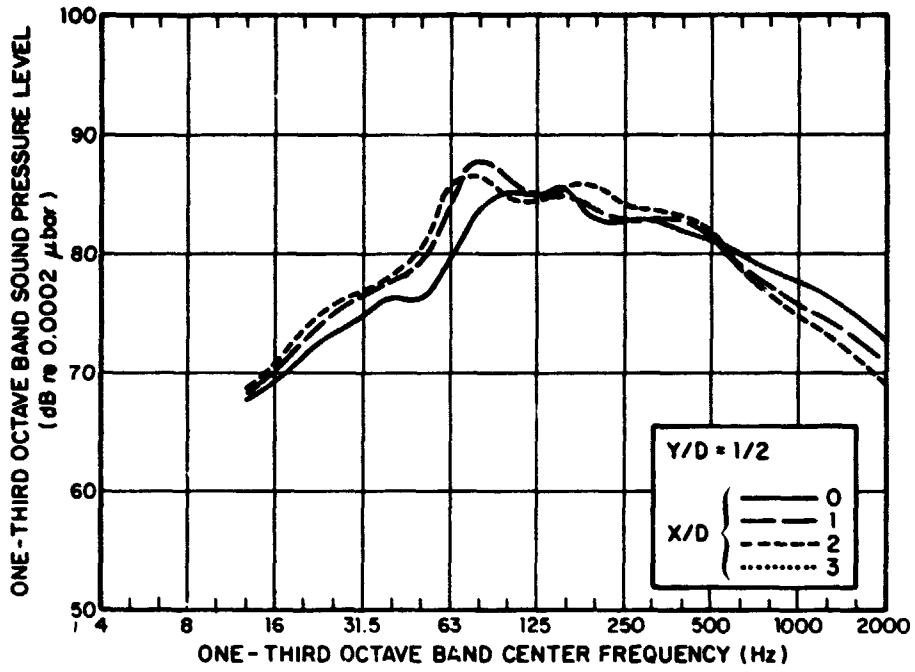


Figure 5.- Flyover noise spectra. Round nozzle; $U_J = 244$ m/sec (800 ft/sec); $U_\infty = 44$ m/sec (145 ft/sec).

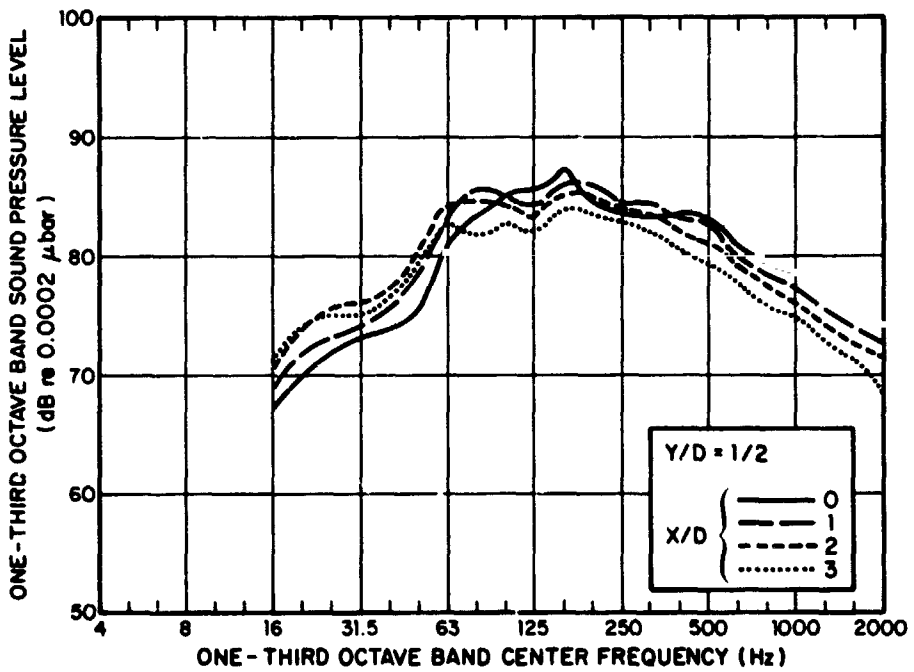


Figure 6.- Flyover noise spectra. Rectangular nozzle; $U_J = 244$ m/sec (800 ft/sec); $U_\infty = 44$ m/sec (145 ft/sec).

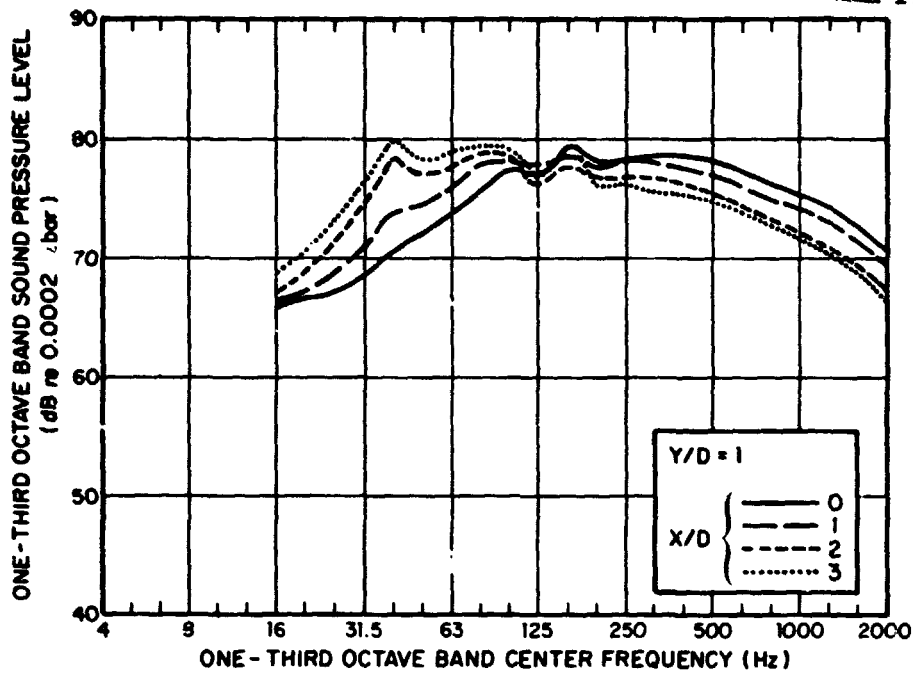


Figure 7.- Sideline noise spectra. Rectangular nozzle; $U_j = 244$ m/sec (800 ft/sec); $U_\infty = 44$ m/sec (145 ft/sec).

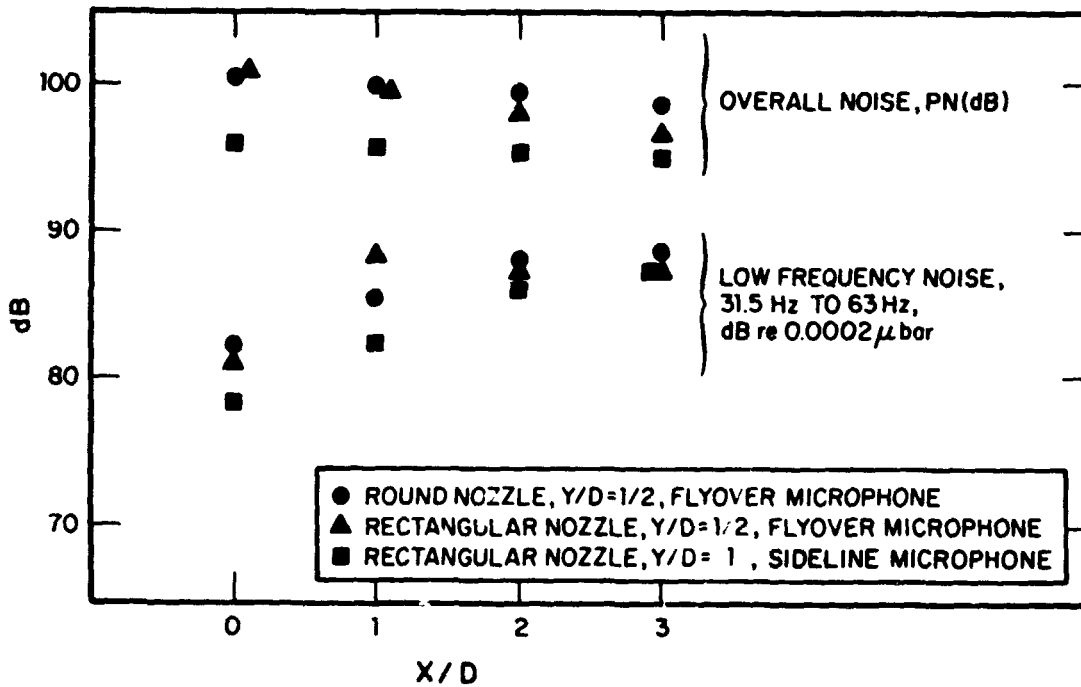


Figure 8.- X/D dependence of overall and low frequency noise; no forward speed.

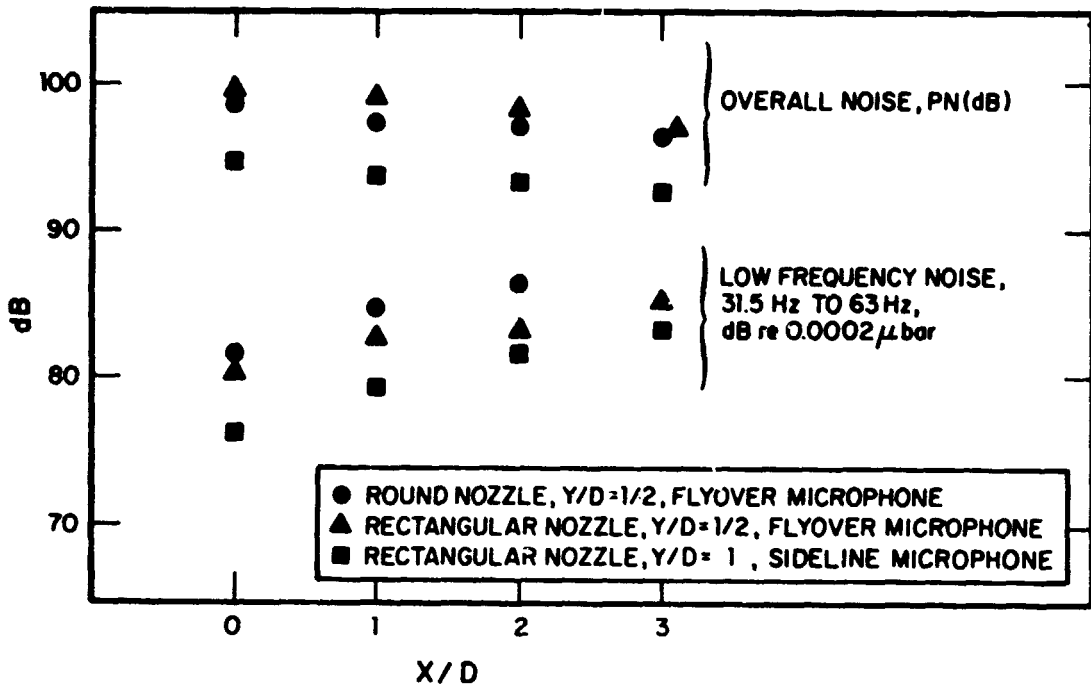


Figure 9.- X/D dependence of overall and low frequency noise; $J_\infty = 44 \text{ m/sec (145 ft/sec)}$.

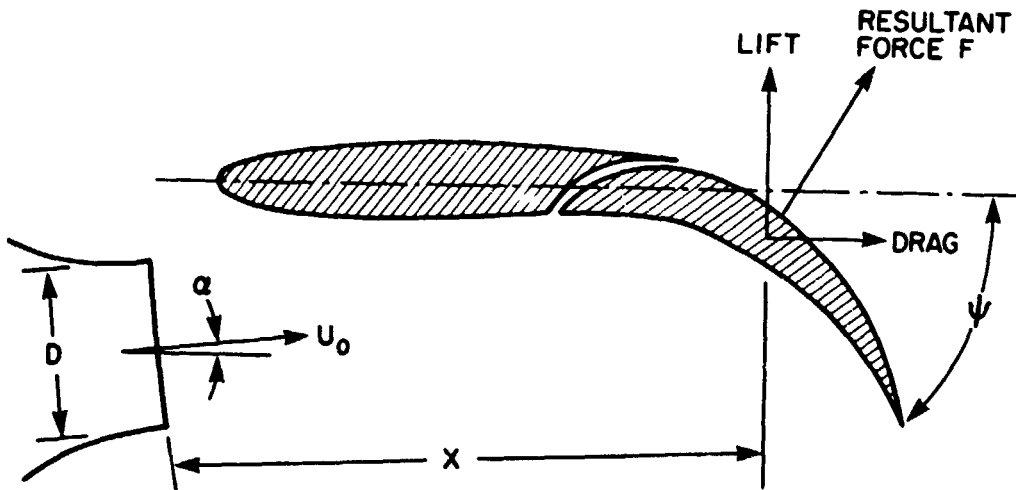


Figure 10.- Externally blown flap as a smoothly faired corner.

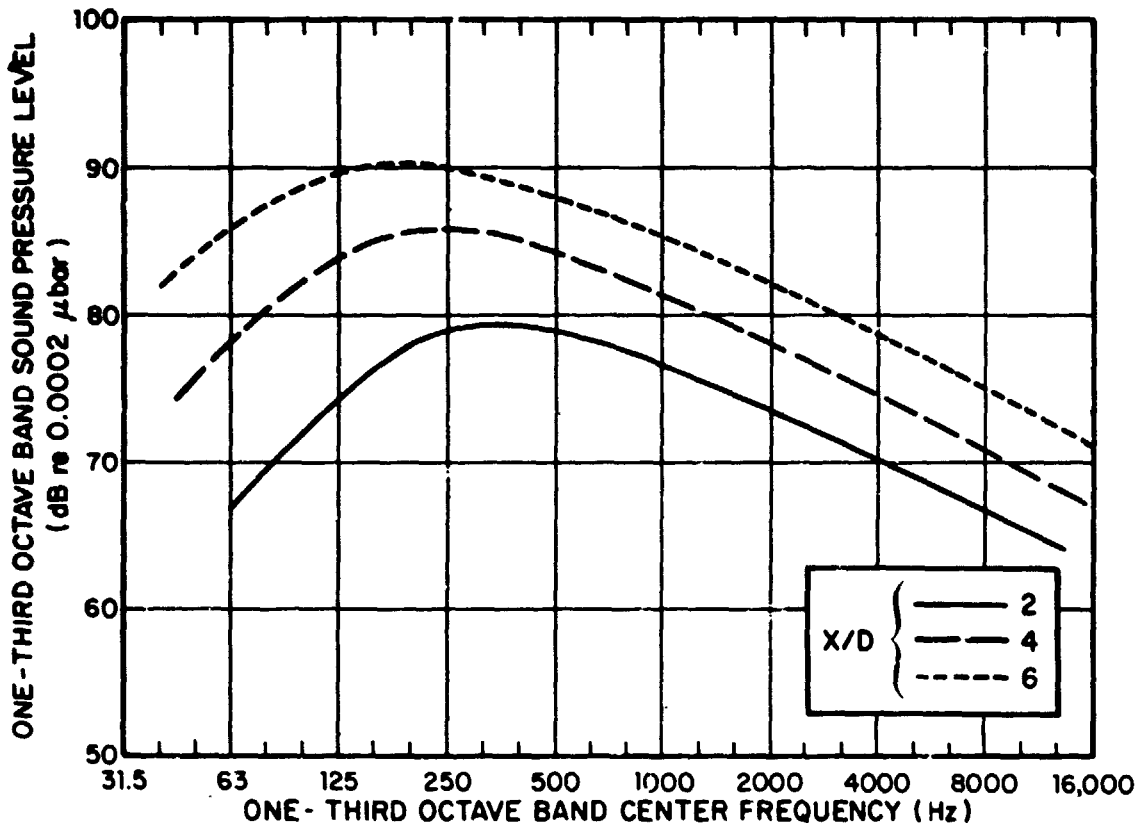


Figure 11.- Estimated noise from fluctuations in gross turning forces.

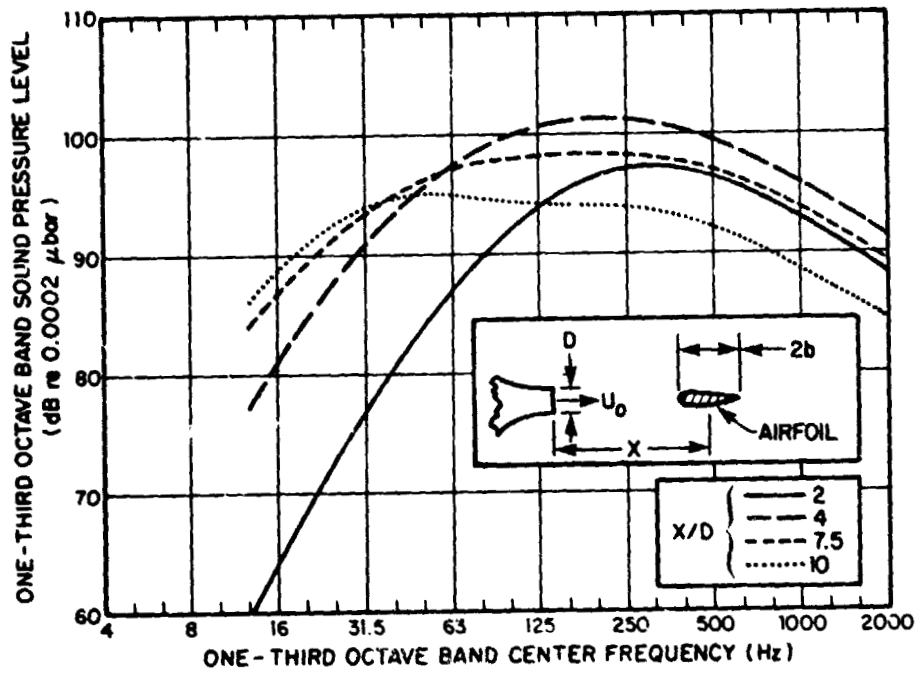


Figure 12.- Estimated noise from fluctuating lift at leading edge.

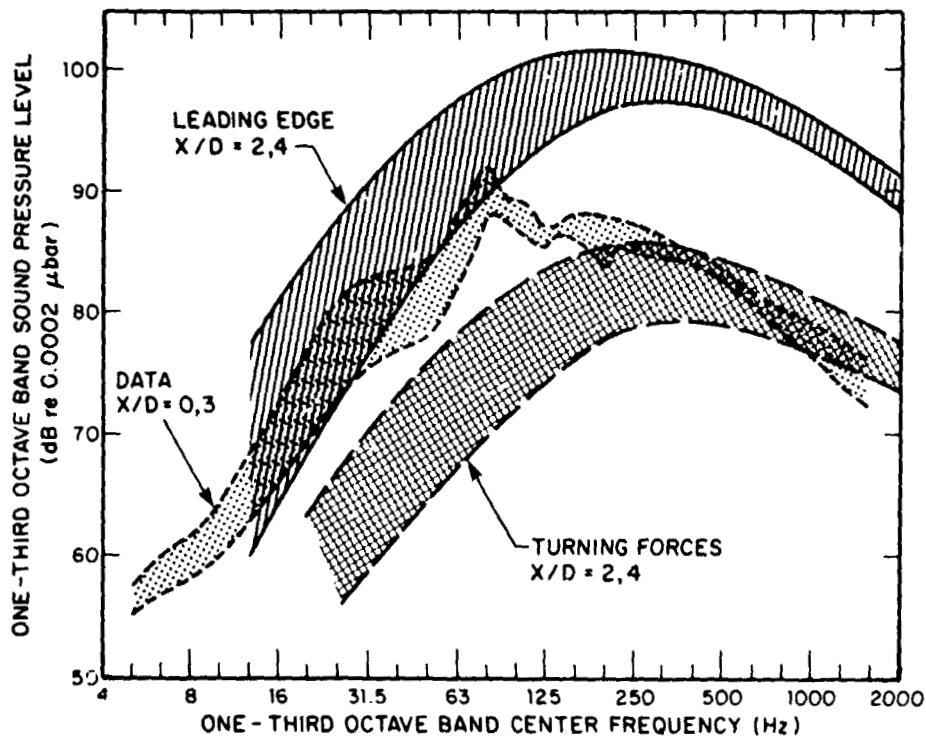


Figure 13.- Comparison of estimated noise and experimental data.